



RESEARCH ARTICLE

Integrative systems immunology uncovers molecular networks of the cell cycle that stratify COVID-19 severity

Caroline Aliane de Souza Prado¹ | Dennyson Leandro M. Fonseca² | Youvika Singh¹ | Igor Salerno Filgueiras³ | Gabriela Crispim Baiocchi³ | Desirée Rodrigues Praça¹  | Alexandre H. C. Marques¹ | Raquel Costa Silva Dantas-Komatsu⁴ | Júlia N. Usuda¹ | Paula Paccielli Freire³ | Ranieri Coelho Salgado³ | Sarah Maria da Silva Napoleao³ | Rodrigo Nalio Ramos^{5,6} | Vanderson Rocha^{5,6,7,8} | Guangyan Zhou⁹ | Rusan Catar¹⁰ | Guido Moll^{10,11} | Niels Olsen Saraiva Camara³ | Gustavo Cabral de Miranda³ | Vera Lúcia Garcia Calich³ | Lasse M. Giiil¹² | Neha Mishra¹³ | Florian Tran^{13,14} | Andre Ducati Luchessi¹⁵ | Helder I. Nakaya^{1,16} | Hans D. Ochs¹⁷ | Igor Jurisica^{18,19,20,21} | Lena F. Schimke³ | Otavio Cabral-Marques^{1,2,3,22,23,24} 

¹Department of Clinical and Toxicological Analyses, School of Pharmaceutical Sciences, University of São Paulo, São Paulo, Brazil

²Interunit Postgraduate Program on Bioinformatics, Institute of Mathematics and Statistics (IME), University of São Paulo (USP), São Paulo, Brazil

³Department of Immunology, Institute of Biomedical Sciences, University of São Paulo, São Paulo, Brazil

⁴Postgraduate Program in Health Sciences, Federal University of Rio Grande do Norte, Natal, Brazil

⁵Laboratory of Medical Investigation in Pathogenesis and Directed Therapy in Onco-Immuno-Hematology (LIM-31), Department of Hematology and Cell Therapy, Hospital das Clínicas HCFMUSP, Faculdade de Medicina, University of São Paulo, São Paulo, Brazil

⁶Instituto D'Or de Ensino e Pesquisa, Hospital São Luiz, São Paulo, Brazil

⁷Fundação Pró-Sangue-Hemocentro de São Paulo, Hospital das Clínicas da Universidade de São Paulo, São Paulo, Brazil

⁸Department of Hematology, Churchill Hospital, University of Oxford, Oxford, UK

⁹Institute of Parasitology, McGill University, Montreal, Quebec, Canada

¹⁰Department of Nephrology and Internal Intensive Care Medicine, Charité University Hospital, Berlin, Germany

¹¹Berlin Institute of Health (BIH) and Berlin Center for Regenerative Therapies (BCRT), Freie Universität Berlin, Humboldt-Universität zu Berlin and Berlin-Brandenburg School for Regenerative Therapies (BSRT), all Charité Universitätsmedizin Berlin, Berlin, Germany

¹²Department of Internal Medicine, Haraldsplass Deaconess Hospital, Bergen, Norway

¹³Institute of Clinical Molecular Biology, Kiel University and University Medical Center Schleswig-Holstein, Kiel, Germany

¹⁴Department of Internal Medicine I, University Medical Center Schleswig-Holstein, Kiel, Germany

¹⁵Department of Clinical and Toxicology Analysis, Federal University of Rio Grande do Norte, Natal, Brazil

¹⁶Instituto Israelita de Ensino e Pesquisa Albert Einstein, Hospital Israelita Albert Einstein, São Paulo, Brazil

¹⁷Department of Pediatrics, University of Washington School of Medicine and Seattle Children's Research Institute, Seattle, Washington, USA

¹⁸Osteoarthritis Research Program, Division of Orthopedic Surgery, Schroeder Arthritis Institute, UHN, Toronto, Ontario, Canada

¹⁹Institute of Neuroimmunology, Slovak Academy of Sciences, Bratislava, Slovakia

²⁰Departments of Medical Biophysics and Computer Science, Faculty of Dentistry, University of Toronto, Toronto, Ontario, Canada

²¹Krembil Research Institute, UHN, Data Science Discovery Centre, Toronto, Ontario, Canada

Lena F. Schimke and Otavio Cabral-Marques contributed equally to this study.

This is an open access article under the terms of the Creative Commons Attribution-NonCommercial-NoDerivs License, which permits use and distribution in any medium, provided the original work is properly cited, the use is non-commercial and no modifications or adaptations are made.

© 2023 The Authors. *Journal of Medical Virology* published by Wiley Periodicals LLC.

²²Department of Pharmacy and Postgraduate Program of Health and Science, Federal University of Rio Grande do Norte, Natal, Brazil

²³Department of Medicine, Division of Molecular Medicine, University of São Paulo School of Medicine, São Paulo, Brazil

²⁴Laboratory of Medical Investigation 29, University of São Paulo School of Medicine, São Paulo, Brazil

Correspondence

Lena F. Schimke and Otavio Cabral-Marques,
Department of Immunology, Institute of
Biomedical Sciences, University of São Paulo,
São Paulo, Brazil.

Email: lenaschimke@usp.br and
otavio.cmarques@usp.br

Funding information

FAPESP, Grant/Award Numbers: 2018/18886-9, 2020/01688-0, 2020/07069-0, 2020/09146-1, 2020/11710-2, 2020/16246-2, 2020/07972-1; Natural Sciences Research Council, Grant/Award Numbers: NSERC#203475, #29272, #225404, #33536; Canada Foundation for Innovation; Coordenação de Aperfeiçoamento de Pessoal de Nível Superior; Conselho Nacional de Desenvolvimento Científico e Tecnológico; German Federal Ministry of Education and Research; Deutsche Forschungsgemeinschaft; German Research Foundation; National Council for Scientific and Technological Development, Grant/Award Number: 102430/2022-5; Ontario Research Fund, Grant/Award Number: #34876; European Union's Horizon 2020 research and innovation program, Grant/Award Numbers: 733006 (PACE), 779293 (HIPGEN)

Abstract

Several perturbations in the number of peripheral blood leukocytes, such as neutrophilia and lymphopenia associated with Coronavirus disease 2019 (COVID-19) severity, point to systemic molecular cell cycle alterations during severe acute respiratory syndrome coronavirus-2 (SARS-CoV-2) infection. However, the landscape of cell cycle alterations in COVID-19 remains primarily unexplored. Here, we performed an integrative systems immunology analysis of publicly available proteome and transcriptome data to characterize global changes in the cell cycle signature of COVID-19 patients. We found significantly enriched cell cycle-associated gene co-expression modules and an interconnected network of cell cycle-associated differentially expressed proteins (DEPs) and genes (DEGs) by integrating the molecular data of 1469 individuals (981 SARS-CoV-2 infected patients and 488 controls [either healthy controls or individuals with other respiratory illnesses]). Among these DEPs and DEGs are several cyclins, cell division cycles, cyclin-dependent kinases, and mini-chromosome maintenance proteins. COVID-19 patients partially shared the expression pattern of some cell cycle-associated genes with other respiratory illnesses but exhibited some specific differential features. Notably, the cell cycle signature predominated in the patients' blood leukocytes (B, T, and natural killer cells) and was associated with COVID-19 severity and disease trajectories. These results provide a unique global understanding of distinct alterations in cell cycle-associated molecules in COVID-19 patients, suggesting new putative pathways for therapeutic intervention.

KEYWORDS

cell cycle associated molecules, COVID-19 severity, proteomics, SARS-CoV-2, systems immunology, transcriptomics

1 | INTRODUCTION

Although more than 12.8 billion vaccine doses have been administered worldwide (as of October 10, 2022, WHO Coronavirus disease 2019 [COVID-19] dashboard), resulting in a substantial reduction of case fatality rates,¹⁻³ new escape variants of severe acute respiratory syndrome coronavirus 2 (SARS-CoV-2) continue to represent a significant challenge to global health. Indeed, recent reports estimate that approximately 2000 daily deaths worldwide can be attributed to COVID-19.⁴ This threat to human health presents a continued medical need to understand better the specific host immunological mechanisms underlying SARS-CoV-2 infection and identify new therapeutic targets.^{5,6}

Patients with severe COVID-19 have a systemically altered innate and adaptive immune response, characterized by hyperactivation of both myeloid and lymphoid cells⁷⁻¹¹ and the production of high circulating autoantibody levels.^{12,13} Moreover, the altered composition of

granulocyte (sub)-populations (neutrophilia and a marked decrease of eosinophils and basophils), the emergence of immature neutrophils in peripheral blood,¹⁴ as well as a profound lymphopenia (CD4⁺ and CD8⁺ T cells, B cells, and natural killer [NK] cells) have been linked to more severe illness. These observations suggest alterations in the molecular mechanisms that orchestrate cell production and proliferation, including cell cycle-associated events that remain poorly characterized. For instance, distinct phosphoproteomics perturbations of cell cycle-associated molecules in SARS-CoV-2-infected cells point to cell cycle inhibitors as a potential therapy for COVID-19 patients.¹⁵ Thus, demanding a comprehensive understanding of the molecular alterations during SARS-CoV-2 infection in humans.

Viruses utilize diverse strategies and molecular targets to create favorable conditions for replication,^{16,17} for example, by interfering with the host cell cycle processes.^{18,19} Viruses such as influenza, herpes, and coronaviruses (SARS-CoV-2 and murine coronavirus/

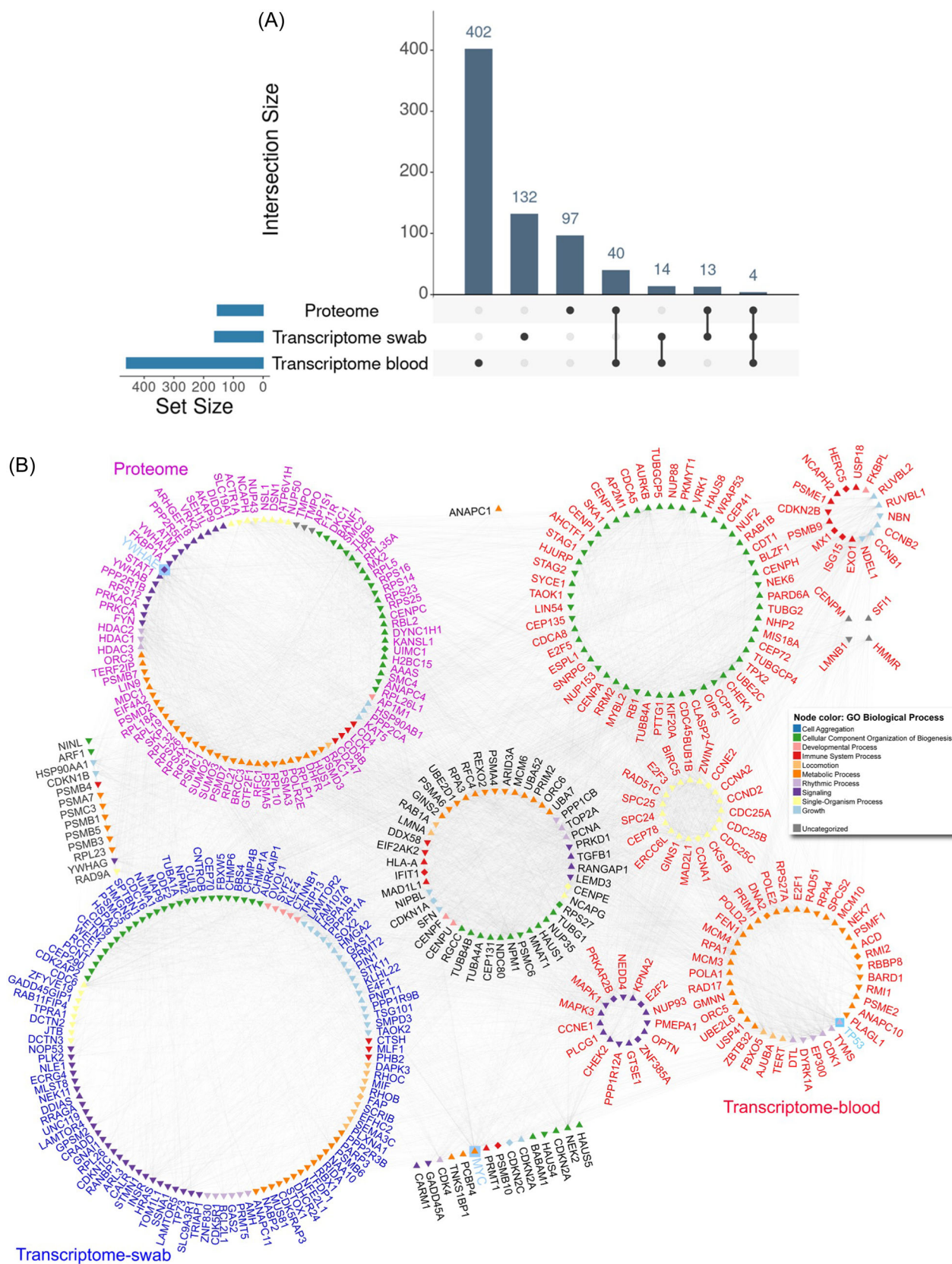


FIGURE 1 (See caption on next page)

mouse hepatitis virus) intervene at different cell cycle checkpoints either by promoting or arresting cell cycle progression, or by disrupting protein synthesis (G0/G1 transition), DNA duplication (G1/S phase), or cell division (G2/M phase).^{20–22} Based on these observations, we hypothesized that SARS-CoV-2 infection induces systemic changes in cell cycle-associated molecules during COVID-19 infection that associate with disease outcome, a hypothesis we investigated in detail using a systems biology approach.

2 | MATERIALS AND METHODS

2.1 | Transcriptomic data curation and differential gene expression analysis

For human transcriptome data, we searched in the Gene Expression Omnibus public genomics data repository (GEO; <https://www.ncbi.nlm.nih.gov/geo/>) from patients with COVID-19, published between December 2019 and January 2021 (Supporting Information: Table Si). Study selection was performed as described earlier,²³ following meta-analysis guidelines to achieve integrative analyses.^{24,25} This search resulted in a total of five data sets, including two transcriptome data sets derived from peripheral blood mononuclear cells (PBMCs) (GSE152418 and GSE161731), one from whole peripheral blood leukocytes (PBLs) (GSE157103), and two from nasopharyngeal swabs (GSE152075 and GSE156063). In total, transcriptome data from 717 COVID-19 samples and 359 non-COVID-19 samples (including healthy controls [HCs] and patients with other infectious diseases) were included in this analysis (Supporting Information: Figure 1b; first square). Read counts were transformed in log2 counts per million, and differentially expressed genes (DEGs) between groups were identified using the DESeq. 2 pipeline²⁶ through the NetworkAnalyst 3.0 bioinformatics platform. References for all R packages and bioinformatic tools used in this study are listed in Supporting Information: Table Sii. The DEGs of each data set were determined by applying the statistical cutoffs of log2 fold-change >1 (upregulated), Log2 fold change < -1 (downregulated), and adjusted *p*-value <0.05. Shared DEGs across different data sets were displayed using Upset plot and Circos plot online web tools.

2.2 | Proteomic data collection and analysis

Proteomic data from plasma, serum, PBMCs, and swab samples from COVID-19 and non-COVID-19 individuals were selected from

previously reported studies (Supporting Information: Table Si). These data are available at Proteome X change (<http://www.proteomexchange.org/>; identifier: PXD020601, PXD022889) or iProX (integrated Proteome resources; identifier: IPX0002285000) or from the supplementary data of Akgun et al.²⁷ Our proteome analysis included 191 COVID-19 samples and 71 non-COVID-19 samples (Supporting Information: Table Si and Figure 1b; second square). The raw protein abundance values were quantified, normalized and log2 transformed. Differences in protein expression between COVID-19 patients and non-COVID-19 individuals were calculated using Fisher's method²⁸ using the Perseus computational platform for comprehensive proteomics data analysis. We considered a cut-off of *p*-value <0.05 and Log2 fold change of >0.5 and <-0.5 for differentially expressed proteins (DEPs).

2.3 | Interactome analysis

For comprehensive network and interactome analyses, we used Integrated Interactions Database IID (version 2021-05) and NAViGaTOR software (version 3.0.16) to build a network visualizing physical protein-protein interactions between the cell cycle-associated genes and proteins obtained from our omics analysis. The cell cycle-associated molecules (Supporting Information: Table S1) were used as input into the Integrated Interactions Database (IID ver. 2021-05; <http://ophid.utoronto.ca/iid>) to identify direct physical protein interactions. The resulting network was annotated, analyzed, and visualized using the NAViGaTOR ver. 3.0.16. The final network was combined with legends using Adobe Illustrator ver. 26.5.

2.4 | Functional enrichment and analysis and identification of gene co-expression modules

To perform enrichment analysis for different sets of DEGs, we used the ClusterProfiler R package in R studio Version 1.4.1106 (Rstudio; <https://www.rstudio.com>) and enrichr online tool. The enrichment analysis of significant proteins was performed using the ShinyGO tool. Sets of cell cycle-associated DEGs and DEPs were visualized in bubble-based heatmaps applying a minus cosine similarity using the Morpheus web tool. Circular heatmaps representing each cell cycle phase were generated using the circlize R package in R studio. In addition, gene co-expression modules were analyzed through the CEMiTool R package using default parameters.

FIGURE 1 Interactive network of multi-omics data integration of cell cycle-associated molecules. (A) Upset plot showing the intersection of transcriptomic (swab and blood) and proteomic data obtained from all studies included in this work. (B) Network of cell cycle-associated molecules from proteome and transcriptome data sets from COVID-19 patients. The color of the nodes represents gene ontology (GO) biological processes according to the figure legend. The genes labeled in red represent the differentially expressed genes (DEGs) from blood transcriptome data sets. DEGs from swab transcriptomes are denoted in the dark blue, and differentially expressed genes (DEPs) from the proteome data sets are labeled in purple. Molecules overlapping in the transcriptomics and proteomics data sets are exhibited in black. Triangles pointing up represent upregulated molecules, triangles pointing down indicate downregulated molecules, and the diamond shape shows DEGs and DEPs upregulated or downregulated across different data sets. The whole network comprises 429 proteins and 10 516 direct physical interactions.

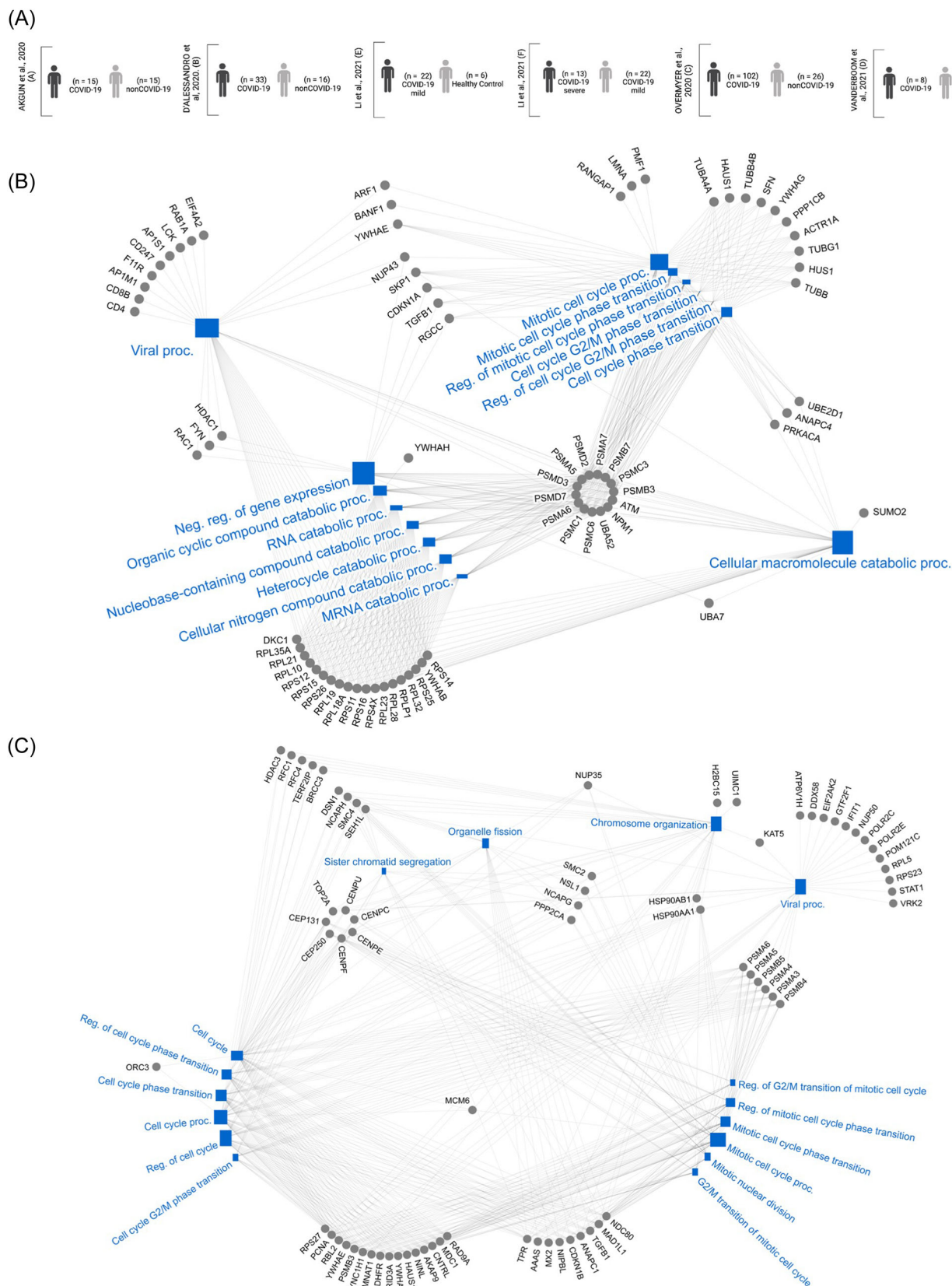


FIGURE 2 Systems-level view of proteome changes related to the cell cycle. (A) Schematic overview showing the number and classification of patient and control cohorts of each data set used for the proteomic data analysis. (B and C) Network of cell cycle-associated proteins (gray nodes) obtained across the study cohorts and biological processes (BPs; blue nodes) enriched by (B) upregulated or (C) downregulated differentially expressed genes (DEPs). Gray edges reflect the association between DEPs and BPs. The interaction network was visualized using NAViGaTOR. More prominent nodes represent larger gene sets. The size of the squares increases according to the number of proteins enriching each BP.

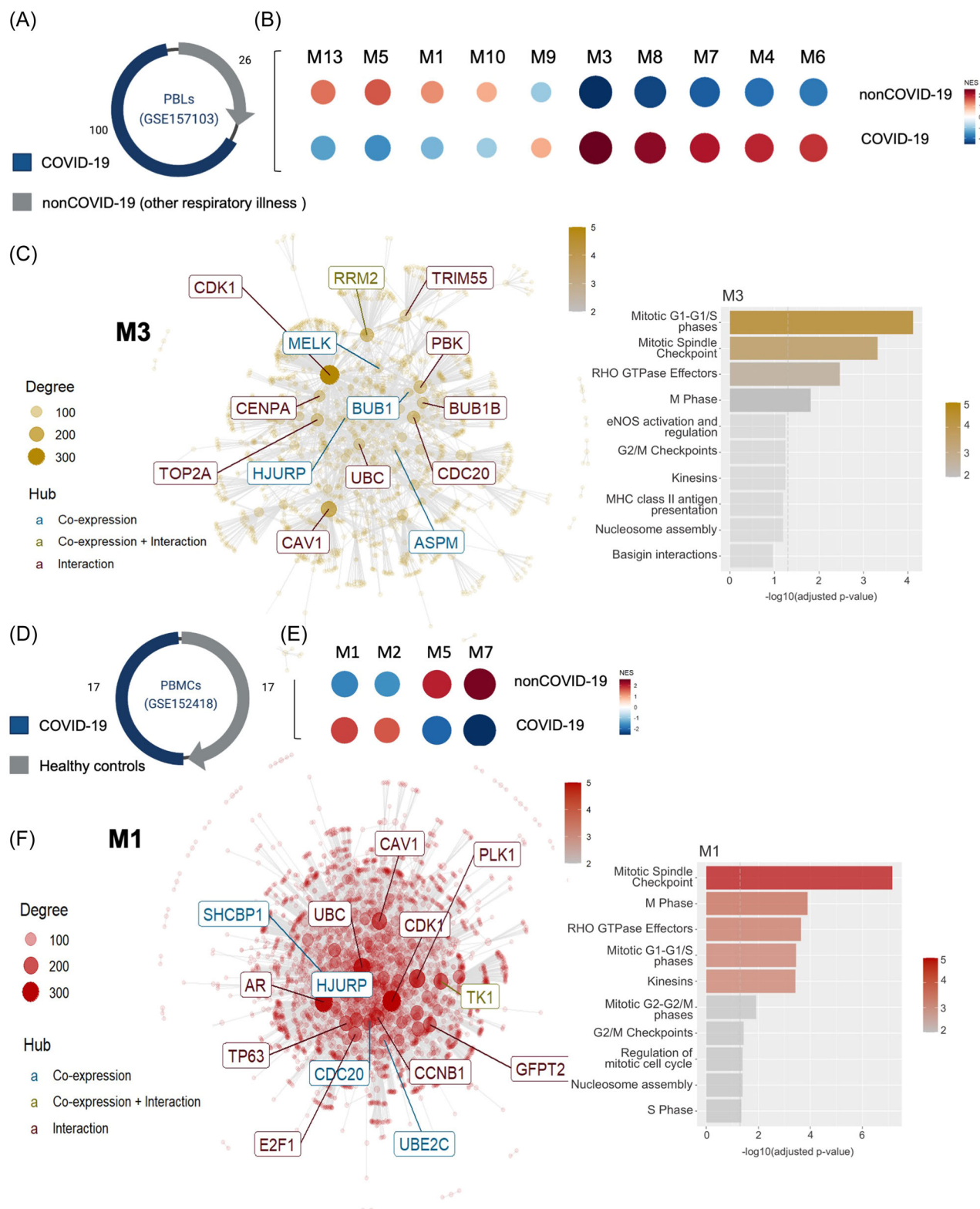


FIGURE 3 Cell cycle-associated gene co-expression modules present in blood transcriptomes of COVID-19 patients. (A) Schematic figure showing the number of samples of the peripheral blood leukocyte (PBL) transcriptome data set (GSE157103) and (D) the peripheral blood mononuclear cells (PBMCs) transcriptome data set (GSE152418). Bubble heatmap showing the results of gene set enrichment analysis, indicating the module (M) activity in (B) COVID-19 patients versus non-COVID-19 (patients with other respiratory illnesses) and (E) COVID-19 patients compared with healthy controls. Circle size and color reflect the normalized enrichment score (NES), as determined by CEMiTool. (C) Interaction plot for M3 (GSE157103) and (F) M1 (GSE152418), which contains genes enriching different cell cycle-associated pathways, exhibited by the bar plot at the right side of figure (C) and (F). The most connected genes (hubs) are highlighted inside rectangles. The node size is proportional to its degree of interactivity. The bar plot indicates the top 10 enriched pathways from the over-representation analysis of module M3 (C) and M1 (F).

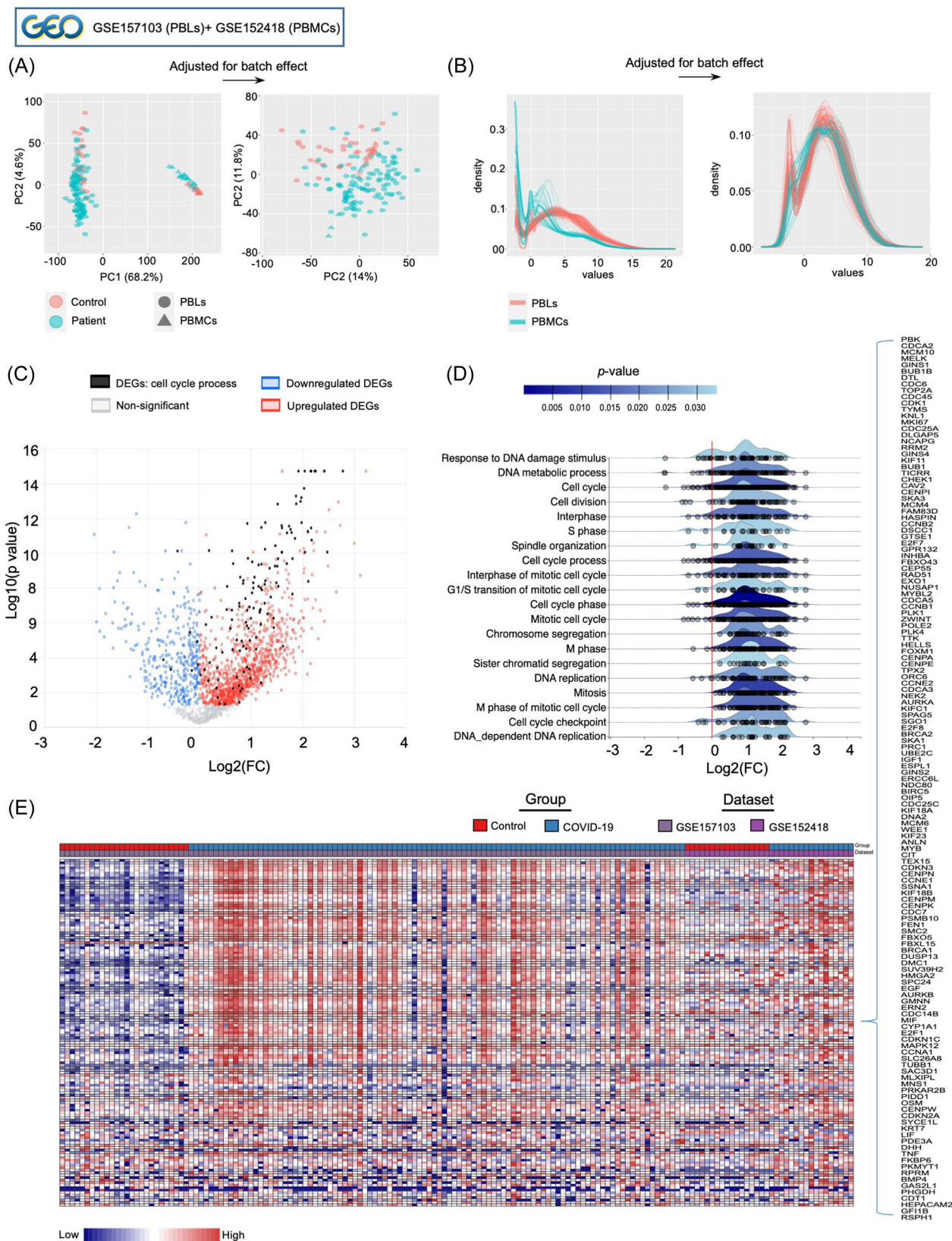


FIGURE 4 (See caption on next page)

2.5 | Meta-analysis of gene expression data sets

Using default parameters, a comprehensive meta-analysis of gene expression data sets was carried out through NetworkAnalyst 3.0. Briefly, the GSE157103 and GSE152418 data sets were adjusted for batch effect, and meta-DEGs were visualized by principal component analysis (PCA) and density plots. We used Fisher's method to obtain combined *p*-values for information integration. We used a volcano plot and Ridgeline chart to display the meta-DEGs and visualized their fold-change distribution across enriched pathways, respectively. Gene expression distribution was based on average Log2 fold change. A hierarchical clustering heatmap visualized the gene expression patterns associated with the cell cycle process.

2.6 | Single-cell RNA-Seq

COVID-19 single-cell data sets were downloaded from the GEO database (GSE149689, GSE174072, GSE171555, GSE163668, GSE169346, GSE161918) and broad institute (SCP1289) and analyzed separately using the Seurat package (v.4.0.4) in R software (v 4.1.1). These studies contain 159 COVID-19 patients and 70 controls (Supporting Information: Figure 1b; third square). Cells with >200 expressed genes were selected for further analyses. Features expressed in fewer than three cells were removed in the analysis. Cells with <15% unique molecular identifiers derived from the mitochondrial genome were removed. After quality filtration, gene expression matrices were processed through the standard processing pipeline of Seurat. The cutoff for significant DEGs has an adjusted *p*-value < 0.05.

2.7 | The cell cycle-associated meta-DEGs association with disease severity

We used ImpulseDE2, a model of intraindividual variation of DEGs over time²⁹ as previously described³⁰ to characterize cell cycle-associated DEGs significantly expressed along COVID-19 disease trajectory using bulk RNAseq data of cohort 1 from the data set GSE161777 (Supporting Information: Figure 1b; fourth square). We performed a PCA to measure the stratification power of cell cycle-associated DEGs in distinguishing COVID-19 severity in PBMCs, PBLs, and nasopharyngeal swabs using the R functions prcomp and princomp via the factoextra package (PCA in R: prcomp vs. princomp).

Moreover, we employed random forest, a machine learning algorithm, to rank the importance of cell cycle-associated DEGs for discriminating COVID-19 patients according to disease severity (COVID-19_ICU vs. COVID-19_nonICU) and from other severe respiratory illnesses (COVID-19_ICU vs. nonCOVID-19_ICU) as previously described.¹² We trained the random forest model using the functionalities of the R package randomForest (version 4.6.14). Five thousand trees were used, and three variables were resampled. Follow-up analysis was conducted with the Gini decrease, number of nodes, and mean minimum depth as criteria to determine variable importance. The adequacy of the random forest model as a classifier was assessed through the out-of-bags (OOBs) error rate and the receiver operating characteristic (ROC) curve. For cross-validation, we split the data set into training and testing sets, using 75% of the observations for training and 25% for testing.

2.8 | Correlation analysis

We used the GSE157103 and GSE152418 data sets to perform correlation analysis between the cell cycle-associated genes, that is, the top 10 meta-DEGs with the highest score predicting COVID-19 severity as obtained in the two random forest analyses. Correlograms were generated with the web tool Intervene (<https://intervene.readthedocs.io/en/latest/index.html>) using Spearman's rank correlation coefficient. Box plots of correlation coefficient distribution were generated using the R packages ggpubr, lemon, and ggplot2 in R studio. Significance was determined using two-sided Wilcoxon rank-sum tests and is indicated by asterisks (**p* ≤ 0.05, ***p* ≤ 0.01, ****p* ≤ 0.001, and *****p* ≤ 0.0001). The correlation index for each gene was obtained as follows: correlation Index = {(positive correlation value) – (negative correlation value)}/number of genes and results obtained visualized by a hierarchical clustering heatmap using the ComplexHeatmap R package as previously reported.¹²

3 | RESULTS

3.1 | Cross-study identification of cell cycle-associated molecules in COVID-19

We performed a cross-study analysis of 9 publicly available data sets, including 1212 individuals. Of those, 808 were SARS-CoV-2 positive,

FIGURE 4 Integrative meta-analysis revealed the predominance of cell cycle enriched pathways in blood leukocytes of COVID-19 patients. This analysis integrated the studies of peripheral blood leukocyte (PBL) (GSE157103) and peripheral blood mononuclear cells (PBMCs) (GSE152418). (A) Principal component analysis (PCA) and (B) density plots show the batch effect adjustment for GSE157103 + GSE152418 through empirical Bayes regression (using ComBat). (C) Meta-analysis results displayed by the volcano plot, which was based on average Log2 fold change (FC) and combined *p*-value obtained using the Fisher's method. Small blue and red circles denote up- and downregulated genes, respectively. Black circles show meta-significant genes associated with the cell cycle process, indicating that they are predominantly upregulated. (D) Ridgeline chart denoting the fold-change distribution of top 20 enriched pathways by the meta-significant genes, suggesting the predominance of cell cycle enriched pathways across the studies. Gene (small gray circles) expression distribution is based on average Log2 FC across the enriched biological process. (E) Interactive heatmap exhibits the expression pattern of significant genes associated with the cell cycle process obtained by the meta-analysis.

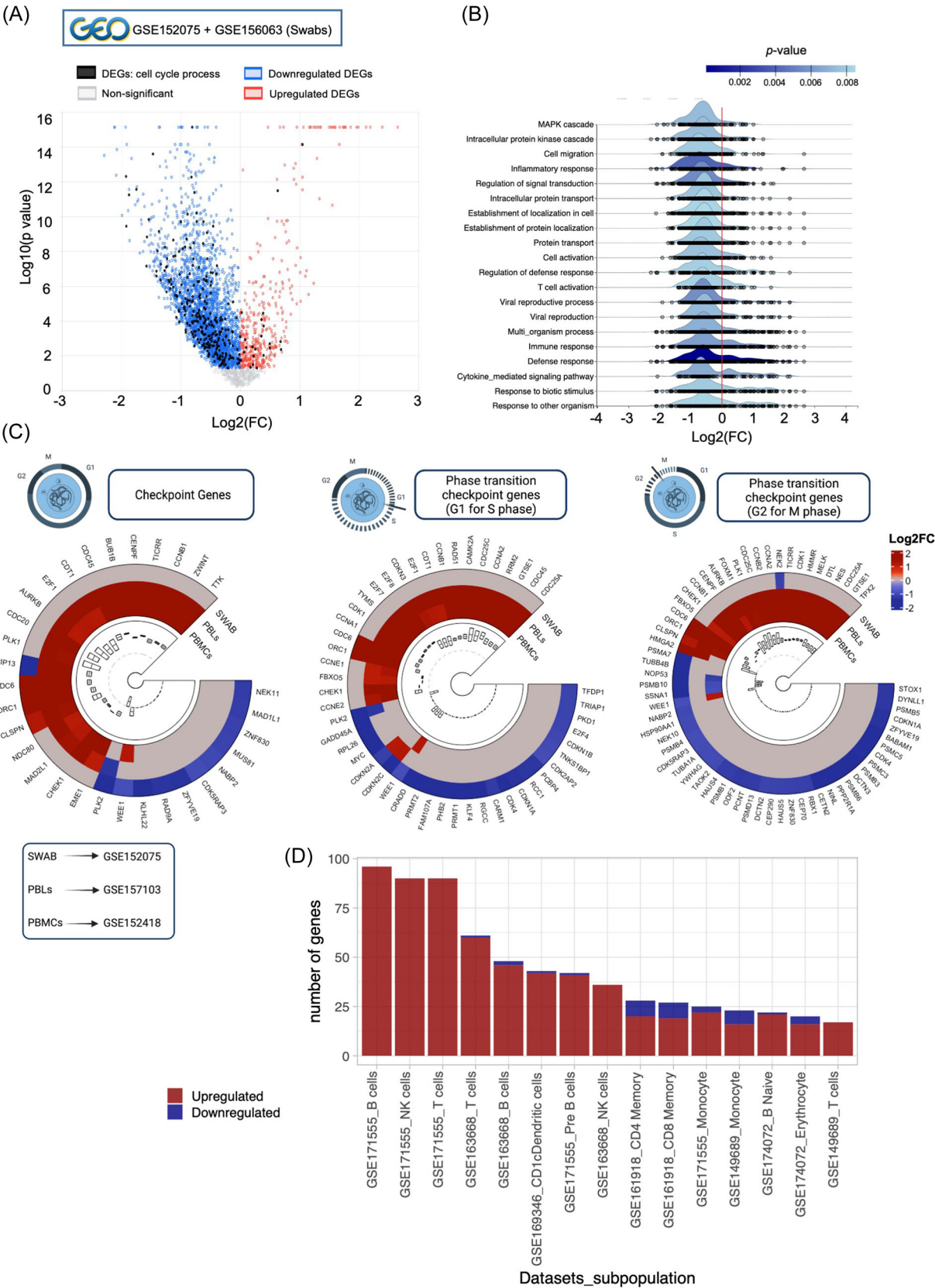


FIGURE 5 (See caption on next page)

and 404 were SARS-CoV-2 negative controls, either healthy or individuals with other respiratory illnesses (Supporting Information: Figure 1b; first and second square box). DEPs were obtained from five proteomic data sets generated by mass spectrometry, each obtained from plasma, serum, and PBMCs, while two used nasopharyngeal swabs. DEGs were obtained from five data sets of bulk-RNA sequencing (RNAseq), one from PBLs, two from PBMCs, and two from nasopharyngeal swabs.

We found 1647 upregulated and 1297 downregulated DEPs, while 10 692 upregulated and 7894 downregulated DEGs across these 9 data sets (Supporting Information: Figure 2a and Table S2). To test our hypothesis, we searched for cell cycle-associated DEPs and DEGs. We found 179 DEPs (89 upregulated and 90 downregulated) and 689 DEGs (437 upregulated and 252 downregulated) that are cell cycle-associated molecules (Supporting Information: Figure 2b and Table S3), including several overlapping upregulated and downregulated DEPs and DEGs across the studies (Figure 1, Supporting Information: Figure 2c and Table S1).

3.2 | SARS-CoV-2 infection systemically changes the expression of cell cycle-associated genes and proteins

Next, we analyzed the proteomic data derived from plasma, serum, PBMCs, and nasopharyngeal swabs obtained from six different cohorts representing five data sets (Figure 2A). This approach revealed that the total number of DEPs and the amount of cell cycle-associated DEPs varied considerably among the data sets studied (Supporting Information: Figure 2 [proteomic data sets] and Tables S2 and S3).

The total DEPs enrich several genetically associated processes such as nucleotide-binding, mRNA processing/splicing, mRNA metabolic processes, and ribonucleoprotein complex (Supporting Information: Figure 3a). The upregulated cell cycle-associated DEPs enrich signaling pathways involved in kinetochore structures, chromosome segregation, mitotic nuclear division, mitotic cell cycle, and organelle organization (Figure 2B and Supporting Information: Figure 3b). Likewise, the downregulated cell cycle-associated DEPs enrich signaling pathways such as those related to the activity of the

proteasome, endopeptidases, ribosomes, and protein catabolic processes (Figure 2C and Supporting Information: Figure 3c). Twenty-four cell cycle-associated DEPs are shared between at least two of the six cohorts (Supporting Information: Figure 3d). While a large amount of cell cycle-associated DEPs is present in PBMC data sets, just a few (less than 10 by data set) are identified in plasma and serum samples of COVID-19 patients, either adults or children (Supporting Information: Table S4).

These results above suggest a systemic change in cell cycle-associated proteins and pathways. We also confirmed this finding at the transcriptional level when carrying out comprehensive modular co-expression analyses to search for sets of co-expressed genes and enriched pathways that are possibly associated with the cell cycle across the blood transcriptome data sets provided by Overmyer et al. (GSE157103) and Arunachalam et al. (GSE152418).^{31,32} Both data sets revealed modules of co-expressed genes that either work together or are similarly (co)-regulated during the immune response to SARS-CoV-2. Among them, modules M3 (Figure 3A-C) and M1 (Figure 3D-F) were significantly upregulated in both PBL (GSE157103) and PBMC (GSE152418) data sets, respectively. Over-representation analysis of these two modules revealed a variety of commonly enriched pathways, including those related to checkpoints such as the mitotic spindle checkpoint and the G2/M checkpoint, as well as other cell cycle-related pathways such as the mitotic G1-G1/S and M phases, and RHO GTPase proteins. These enriched modules contain hubs (most connected genes), also identified among cell cycle-associated DEGs, such as *CDK1*, *CDC20*, *CCNB1*, *TK1*, *PLK1*, *UBE2C*, *E2F1*, *RRM2*, *CENPA*, and *BUB1B*. These findings indicate substantial molecular alterations in the cell cycle during the immune response to SARS-CoV-2.

3.3 | The expression of cell cycle-associated genes predominates in peripheral blood leukocytes of COVID-19 patients

Next, we investigated the transcriptional intersection between DEGs of peripheral blood leukocytes from COVID-19 patients. After adjusting for batch effect (Figure 4A,B), we performed a meta-analysis for the integration of the GSE157103 (PBLs) and

FIGURE 5 Alterations of cell cycle signatures in the blood are not present in transcriptomes from nasopharyngeal swabs of COVID-19 patients. (A) Meta-analysis results displayed by the volcano plot, which is based on average Log2 fold change (FC) and *p*-value from the meta-analysis performed to obtain combine *p*-values from swab transcriptomes (GSE152075 and GSE156063 data sets) using the Fisher's method. Small blue and red circles denote up- and downregulated genes, respectively. Black circles show significant genes that are associated with the cell cycle, indicating that these genes are primarily downregulated in swab transcriptomes. (B) Ridgeline chart denoting the fold-change distribution of the top 20 enriched pathways by the meta-significant genes, indicating the predominance of the inflammatory response, immune and defense activation, while no cell cycle enriched pathways across the swab studies. Gene (small gray circles) expression distribution is based on average Log2 FC across the enriched pathways. (C) Circular heatmaps of a set of genes involved in each phase of the cell cycle in swab and blood (peripheral blood leukocytes [PBLs] and peripheral blood mononuclear cells [PBMCs]) transcriptomes. Color scale refers to up- (red) and downregulated (blue) genes. Gray fields indicate genes not differentially expressed in the data sets (list of all genes described in Supporting Information: Table S9). (D) The number of upregulated cell-cycle associated DEGs across different leukocyte subpopulations from single-cell RNAseq data sets (Supporting Information: Table S11). Each data set's GSE number and cell subpopulations are shown below the bar plot.

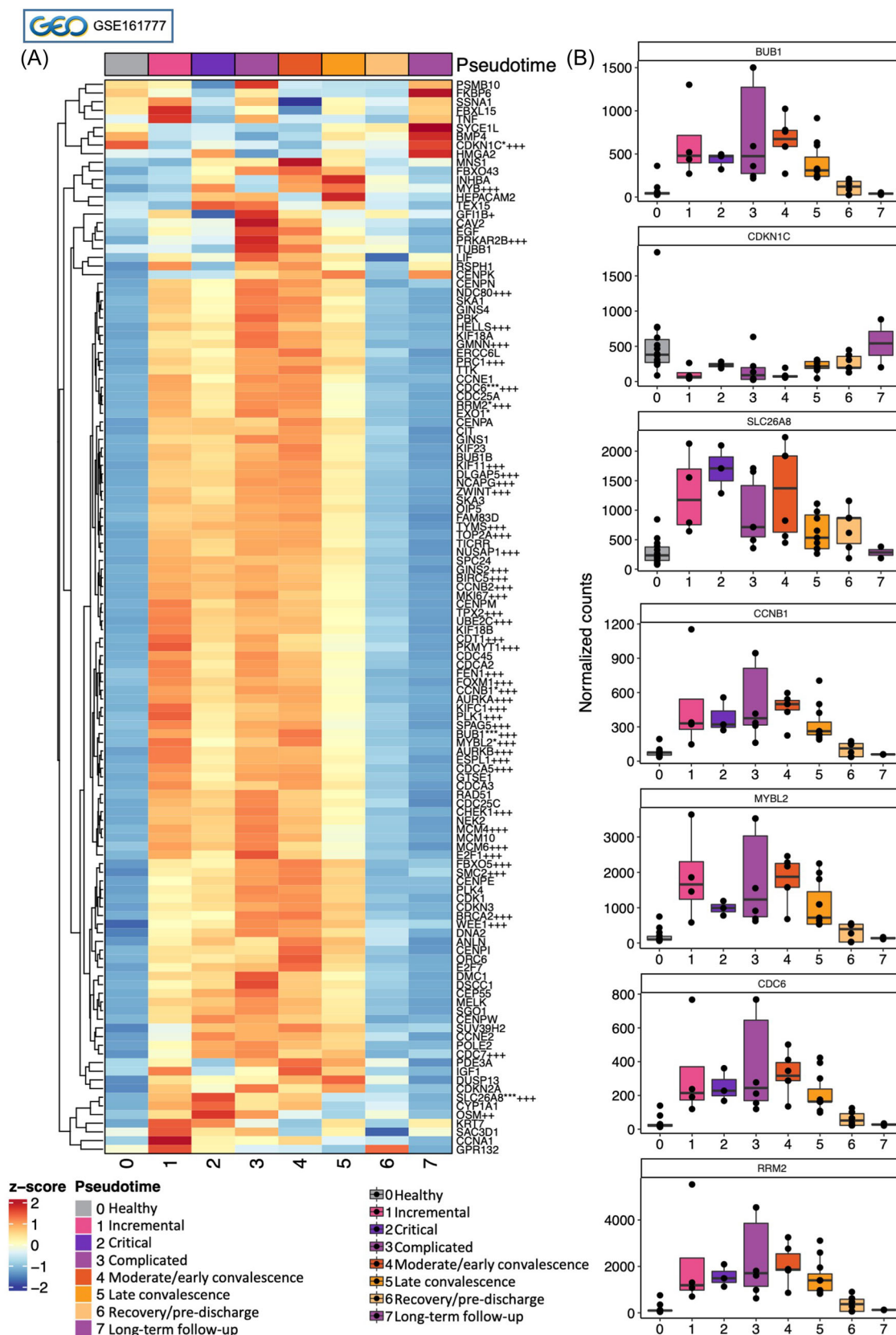


FIGURE 6 (See caption on next page)

GSE152418 (PBMCs) data sets resulting in 1630 meta-DEGs (Figure 4C and Supporting Information: Table S5). Despite the presence of granulocytes (primarily neutrophils) in PBLs but not in PBMCs, enrichment analysis of the meta-DEGs between these leukocyte populations unraveled mostly cell cycle processes among the top 20 enriched biological processes (BPs) (Figure 4D; the complete list of all enriched terms in Supporting Information: Table S6), mainly enriched by upregulated meta-DEGs (Figure 4D).

Among others, the significantly enriched BPs include cell cycle processes, cell division, interphase, S and M phases, G1/S transition of the mitotic cell cycle, cell cycle phase, and cell cycle checkpoints. Figure 4E displays the expression pattern of 126 meta DEGs enriching the cell cycle processes and stages across the GSE157103 and GSE152418 data sets. For instance, among the cell cycle-associated meta-DEGs are those that encode proteins such as cyclin A1 (CCNA1), B1 (CCNB1), B2 (CCNB2), E1 (CCNE1), and E2 (CCNE2). These molecules are essential regulators of mitosis and cell division, forming complexes with their respective cyclin-dependent kinases (CDK1, CDK2, CDK3)³³ and thus regulating and controlling the cell cycle machinery and progression from one to another phase.^{34,35} In addition, cell division cycle (CDC) molecules (CDC25A and CDC25C) and CDK1 were also present as meta-DEGs, which are central actors in cell division interacting with various proteins at various points in the cell cycle.³⁶

3.4 | Compartmentalization of cell cycle signatures in COVID-19 patients

Next, we asked whether the cell cycle signature was specific for peripheral blood leukocytes compared to that in swabs of the upper respiratory tract. To address this issue, we performed a meta-analysis for the integration of transcriptome data from nasopharyngeal swabs obtained from COVID-19 patients versus HCs using the data set GSE152075 and from COVID-19 patients compared with patients who had other viral acute respiratory illnesses (OV-ARIs) or other nonviral ARIs (OnV-ARIs) using the data set GSE156063.

Despite the presence of significant cell cycle-associated DEGs (most of them downregulated) among these studies (Figure 5A, list of all meta-DEGs in Supporting Information: Table S7), this approach revealed no significantly enriched cell cycle-associated pathways

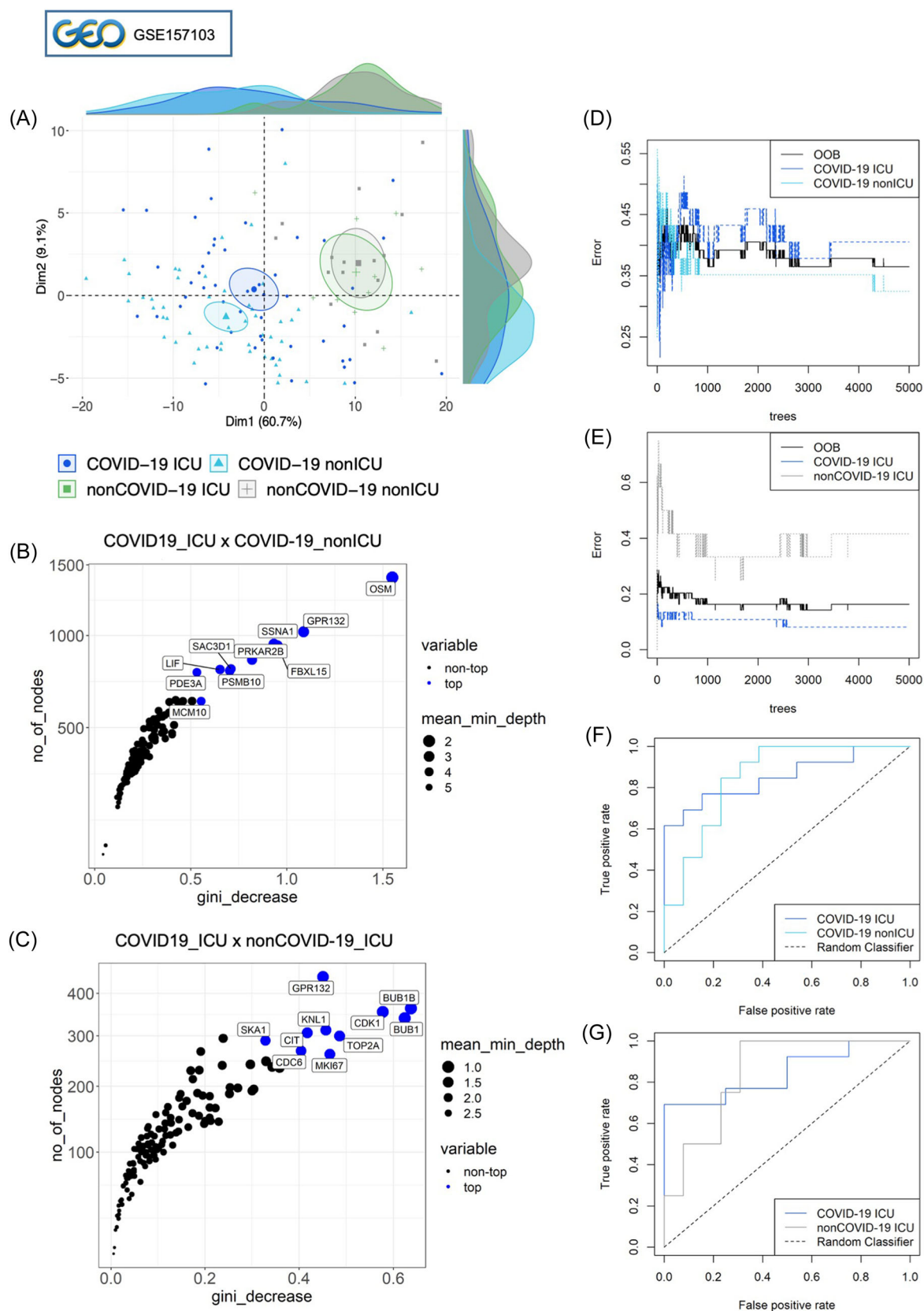
(Figure 5B and Supporting Information: Table S8). The top 20 pathways enriched by the swab meta-DEGs include cell migration, inflammatory response, T cell activation, defense response, and cytokine-mediated signaling pathways. Like the proteomic results, which also show a higher number of cell cycle-associated DEPs in PBMC samples from COVID-19 patients compared to nasopharyngeal swabs (Supporting Information: Figure 2), the bulk RNAseq results indicate the uniqueness of the blood cell-cycle signature. This is further illustrated by the specific upregulation of several checkpoint- and phase transition-related DEGs in the blood but not in the nasopharyngeal swab samples of COVID-19 patients compared to HCs (Figure 5C and Supporting Information: Table S9). Following the bulk RNAseq results, the analysis of scRNAseq data revealed the same phenomena when we searched for the meta-significant cell cycle-associated DEGs in the scRNAseq data sets. Almost none of these meta-DEGs were present as differentially expressed in nasopharyngeal swabs from COVID-19 patients (Supporting Information: Table S10). In contrast, blood lymphocyte subpopulations (B, T, and NK cells) showed the highest number of meta-DEGs associated with the cell cycle signature (Figure 5D and Supporting Information: Table S11).

Nonetheless, we also found a variety of cell-cycle associated DEGs (both upregulated and downregulated) in lung tissue transcriptomes (GSE1822917 and GSE183533) of COVID-19 patients (Supporting Information: Table S12). When comparing lung with blood transcriptomes, we found that they mostly shared upregulated DEGs. In turn, comparing lung tissue with swab transcriptomes revealed common downregulated DEGs (Supporting Information: Figure 4) and also common DEGs that are upregulated in the lung but downregulated in swabs. Thus, future studies are required to investigate further the compartmentalization of the cell cycle signature in COVID-19 patients across different cell types and tissues.

3.5 | The expression of cell cycle-associated meta-DEGs associates with COVID-19 trajectory and disease severity

Considering the relevance of temporal analyses on the dynamics of circulating immune cells in COVID-19 to define predictors of

FIGURE 6 Expression of cell cycle-associated genes upregulates during severe COVID-19 disease phases and normalizes with disease recovery. (A) Heatmap showing the average expression of 126 cell cycle-associated genes (list of genes [see Supporting Information: Table S13] obtained by meta-analysis of peripheral blood leukocyte [PBL]: GSE157103 and peripheral blood mononuclear cells [PBMCs]: GSE152418 data sets) in different disease stages of COVID-19 patients (pseudotimes 0–7 according to figure legend) using the previously published gene expression data from Bernardes et al.³⁰ Row-wise z-scores of the scaled mean expression per pseudotime are plotted and hierarchically clustered in the heatmap. Differentially expressed genes (DEGs) in the longitudinal analysis are denoted with an asterisk (*), and DEGs resulting from the comparison of COVID-19 versus healthy controls are denoted by the + sign according to the adjusted *p*-value (*/+*p* ≤ 0.05, **/+*p* ≤ 0.01, ***/+++*p* ≤ 0.001). (B) Box plots illustrate normalized counts distribution across pseudotimes (0–7) for seven significant genes (significance level shown in (A)). Each box plot shows the median with the first and third interquartile range (IQR), whiskers representing minimum and maximum values within IQR, and individual data points.

**FIGURE 7** (See caption on next page)

disease outcomes,^{30,37,38} we performed a longitudinal study of the cell-cycle associated meta-DEGs across the COVID-19 disease trajectory. We investigated if the meta-DEGs from peripheral blood leukocytes related to the cell cycle process represent markers of severe COVID-19. We first used ImpulseDE2, a model of intraindividual variation of DEGs over time²⁹ using the data set GSE1617777, as previously described.³⁰ We used this approach to find several cell cycle-associated genes significantly differentially expressed in PBLs from COVID-19 patients along the COVID-19 disease trajectory (Figure 6 and Supporting Information: Table S13). These genes are highly expressed during severe COVID-19 phases (disease pseudotimes as characterized by Bernardes et al.³⁰), reducing their expression during disease recovery. For instance, among them, there are several longitudinally cell cycle-associated DEGs such as those previously characterized as potential therapeutic targets (budding uninhibited by benzimidazoles 1 or *BUB1*; Cyclin B1 or *CCNB1*),³³ biomarkers of immune infiltrates (cyclin-dependent kinase inhibitor 1C or *CDKN1C*³⁴; cell division cycle 6 or *CDC6*³⁵; Ribonucleoside-diphosphate reductase subunit or *RRM2*³⁶). We also analyzed whether the cell-cycle associated meta-DEGs stratify COVID-19 patients by disease severity groups and individuals with other respiratory illnesses using the PBL-derived COVID-19 data set (GSE157103). We first performed PCA using a spectral decomposition approach. We found that these meta-DEGs stratified COVID-19 patients that were either admitted or not admitted to the intensive care unit (COVID-19_ICU and COVID-19_nonICU). However, these meta-DEGs did not stratify individuals with other respiratory infections admitted to the ICU and non-ICU (Figure 7A and Supporting Information: Table S14). The severity of illness at ICU admission was defined based on APACHE II and SOFA scores³⁹ according to Overmyer et al.³¹ (Supporting Information: Figure 5). However, although these results indicate that the cell cycle signature of COVID-19 patients is strikingly different from other respiratory illnesses, it also presents a partial overlap with other respiratory illnesses. We identified 28 shared cell cycle-associated DEGs in PBMCs from COVID-19 patients (data set GSE161731) when compared with PBMCs from individuals with bacterial pneumonia, influenza virus, and seasonal coronavirus other than SARS-CoV-2 (sCoV) (Supporting Information: Figure 6). The 28 shared cell cycle-associated DEGs we identified present a similar

expression pattern of upregulation and downregulation across all disease groups compared to HCs.

Furthermore, we performed random forest analysis to identify the most relevant meta-DEGs stratifying COVID-19_ICU from COVID-19_nonICU and COVID-19_ICU from nonCOVID-19_ICU. The random forest model ranked the 10 most crucial cell cycle-associated meta-DEGs for these comparisons based on their ability to discriminate between these disease groups. The analysis identified that *OSM*, *GPR132*, *SSNA1*, *PRKAR2B*, *FBXL15*, *SAC3D1*, *PSMB10*, *LIF*, *PDE3A*, and *MCM10* discriminated COVID19_ICU from COVID-19_nonICU (Figure 7B), while *BUB1B*, *BUB1*, *CDK1*, *TOP2A*, *MKI67*, *CDC6*, *CIT*, *KNL1*, *GPR123*, *SKA1* discriminated COVID19_ICU from nonCOVID19_ICU (Figure 7C and Supporting Information: Table S15).

In this context, Figure 7D,E demonstrates the stable curves based on the number of trees and OOB error rate. Figure 7F,G shows the ROC curves exhibiting the relationship between true and false positive classification rates. Of note, the correlation intensity of the top 10 gene rankers of COVID-19 severity (as in Figure 7B,C) is stronger in COVID-19_ICU patients compared to COVID-19_nonICU, nonCOVID-19_nonICU, and nonCOVID-19_ICU groups. The analysis of correlograms (Figure 8A), correlation coefficient distribution (Figure 8B), and correlation index (Figure 8C) of each of these top-ranked genes across the study cohorts supports this assumption.

4 | DISCUSSION

This work provides a systems immunology view of the network of cell cycle-associated genes and proteins that are involved in the immune response against SARS-CoV-2 infection. We identified multiple distinct changes in the cell-cycle signature of SARS-CoV-2 infected patients, which were associated with COVID-19 severity. The integration of various cohorts revealed a specific network of cell cycle-associated DEPs and DEGs that provide a cell-cycle signature in peripheral blood leukocytes, but not in nasopharyngeal swabs, that distinguishes SARS-CoV-2-infected patients from HCs and patients with other respiratory illnesses. Although we did not linearly characterize mechanisms underlying a specific cell cycle-associated pathway, which represents an essential limitation of this study, our

FIGURE 7 Cell cycle-associated genes stratify COVID-19 from other respiratory illnesses. (A) Principal component analysis (PCA) of meta-significant cell cycle-associated genes (list of genes [see Supporting Information: Table S14] obtained by meta-analysis of peripheral blood leukocyte [PBL]: GSE157103 and peripheral blood mononuclear cells [PBMCs]: GSE152418 data sets) showing the stratification of COVID-19 from non-COVID-19 patients with other respiratory illness (patient cohorts from data set GSE157103 are described in Supporting Information: Figure 4); both groups containing patients admitted to an intensive care unit (ICU) or not (non_ICU). Confidence ellipses are shown for each group. Density plots associated with the PCA indicate the sample distribution across the PCA axes. (B and C) Variable importance score plot obtained by random forest classification analysis. The importance score plot is based on the Gini decrease and number (no.) of nodes for each variable (cell cycle-associated meta-DEGs). It indicates the top 10 variables predicting COVID-19 severity when comparing (B) COVID-19_ICU versus COVID-19_non_ICU and (C) COVID-19_ICU versus non-COVID-19_ICU. Small blue circles show the top 10 gene rankers of COVID-19 severity while the black circles represent those below (with less importance) the top 10. (D and E) Stable curve indicating the number of trees and out-of-bag (OOB) error rate of the random forest analysis. (F and G) Receiver operating characteristic (ROC) curves with an area under the curve (AUC) exhibiting the relationship between true and false positive classification rates.

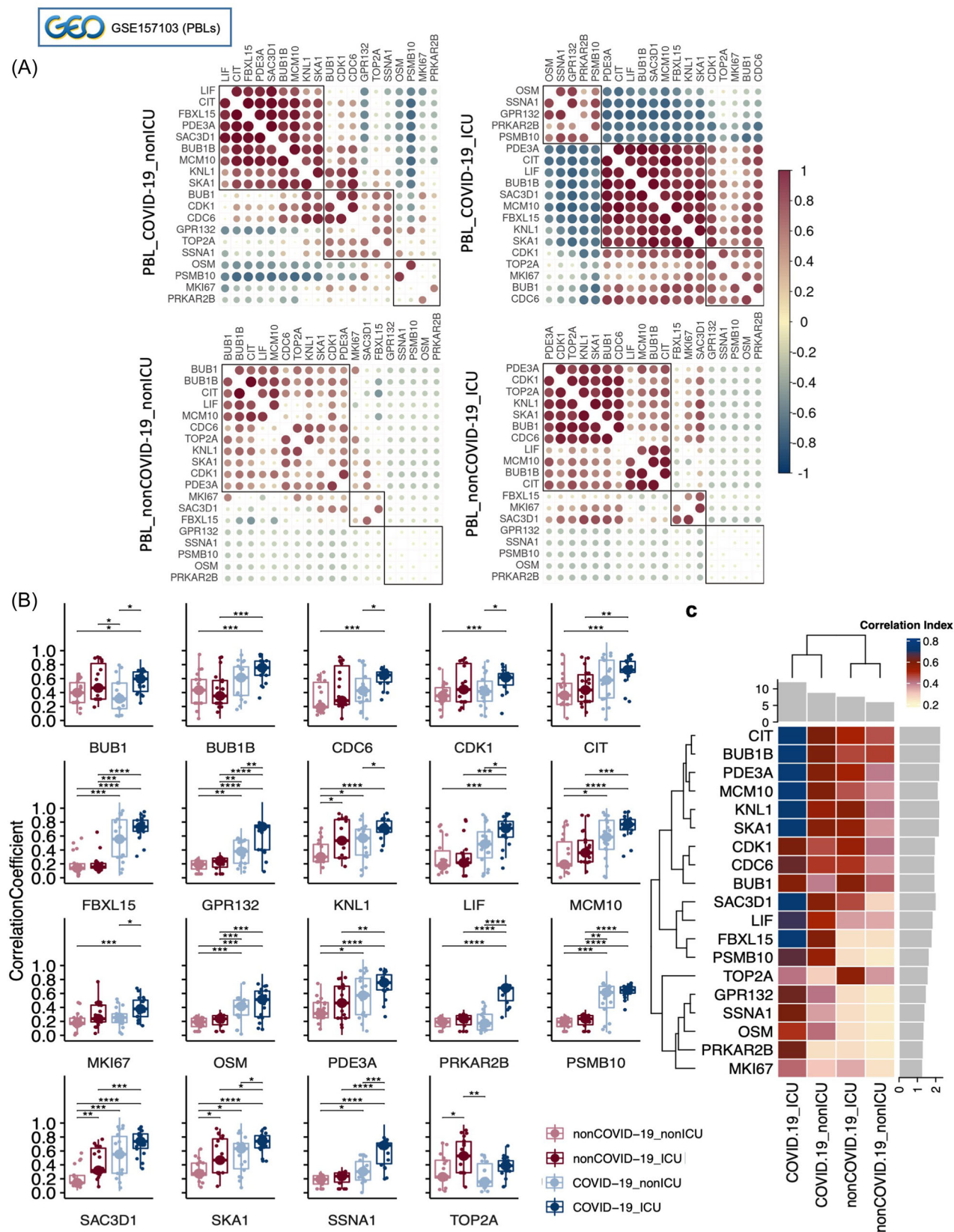


FIGURE 8 (See caption on next page)

findings indicate that SARS-CoV-2 infection triggers multiple systemic changes in the cell-cycle signature of COVID-19 patients.

Recently, an *in vitro* phosphoproteomic study¹⁵ using VeroE6 cells showed that SARS-CoV-2 affects pro-inflammatory cytokine production and the activation of different kinases such as casein kinase II (CK2), CDK, and mitogen-activated protein kinase networks.¹⁵ These proteins play a crucial role in the regulation and progression of cell division.²² These considerations indicate that cell cycle alterations in the immunological signatures of COVID-19 patients are an immunopathological mechanism triggered by the SARS-CoV-2 virus. Accordingly, the modular co-expression analysis we performed revealed modules of co-expressed genes that either work together or are similarly (co)-regulated during the immune response to SARS-CoV-2 across the blood transcriptome data sets. Likewise, meta-analysis for integrating the transcriptome data from peripheral blood leukocyte studies confirmed the predominance of cell cycle enriched pathways regulated during SARS-CoV-2 infection. Our results and the global phosphorylation landscape of SARS-CoV-2 infection reported by Bouhaddou et al.¹⁵ suggest that SARS-CoV-2 systematically affects the cell-cycle machinery, as the severe COVID-19 patients have the highest level of systemic changes in the cell cycle signature of blood cells. Several results presented in our work support this observation. Cell cycle-associated genes of PBLs from COVID-19 patients are highly expressed during severe COVID-19 phases, returning to their normal expression levels during disease recovery.

Of note, the alterations in the cell cycle signatures that occur during the anti-SARS-CoV-2 immune responses are partially not exclusive of the anti-SARS-CoV-2 immune response. Our work suggests a certain degree of overlap with sCoV, influenza virus, and certain bacteria causing pneumonia. This finding indicates that future therapeutic approaches^{22,31} could target cell cycle-associated molecules to develop common potential drugs against different pathogens causing respiratory infections, such as different coronaviruses.⁴⁰ However, although COVID-19 patients share some common cell cycle-associated genes with patients with other respiratory diseases, there is a stratification of patients with SARS-CoV-2 infections based on their total cell cycle-associated signature. In addition, the correlation of the top 10 gene rankers of COVID-19 severity is stronger in COVID-19_ICU patients compared to COVID-19_nonICU patients and those with other respiratory illnesses. These findings indicate that the cell cycle signature might have a more substantial prognostic value for patients with severe SARS-CoV-2 infections. Although this possibility needs further

investigation, it could explain why the increased neutrophil-to-lymphocyte ratio is a more robust prognostic marker for SARS-CoV-2 infections with unfavorable outcomes than for other respiratory illnesses such as influenza.⁴⁰

In this context, the multiple molecular cell-cycle alterations that we identified suggest that SARS-CoV-2 mainly affects human leukocytes, as indicated by our integrative analyses of proteomic, bulk RNAseq, and scRNAseq data. Based on the scRNAseq data, it is likely that the cell-cycle alterations affect predominately B, T, and NK cells, which is expected since proliferation is a fundamental response characteristic for lymphocytes during antigenic stimulation.⁴¹ However, the pathologic effect of SARS-CoV-2 infection results in multiple cellular alterations not only in lymphocytes but also monocytes, eosinophils, and basophils, while neutrophil counts are elevated,⁴² indicating that the changes of cell cycle-associated genes and proteins may not be limited to the peripheral blood. Wang et al.⁴³ reported that bone marrow hematopoietic stem cells from severe COVID-19 patients were dysregulated, prone to apoptosis, and tended to arrest in G1, resulting in diminished lymphocyte progenitors while immature myeloid progenitors accumulated.

However, whether these systemic cell cycle changes represent a hyperactive immune response (e.g., cytokine storm) or an adaptive immune response to the SARS-CoV-2 virus requires future investigation. While the lymphopenia observed in patients with severe COVID-19 disease^{42,44} may counterbalance the effects of the virus-induced cytokine storm, immature myeloid-derived suppressor cells (MDSC) are generated. This heterogeneous group of cells with low oxidative burst activity suppresses T and B lymphocyte responses nonspecifically.⁴⁵ Following the initial hyperactivation of neutrophils in response to SARS-CoV-2 infection, when the severity of COVID-19 advances, the host immune system increases the granulocytic MDSCs production while the number of circulating lymphocytes decreases.^{46–48} MDSCs are a component of the healthy immune system and play a protective role during immune homeostasis and disease context. Specifically, MDSCs expand to reduce tissue damage during autoimmune and inflammatory diseases,⁴⁹ suggesting a physiological role for the systemic cell cycle changes underlying the neutrophilia associated with an increased number of MDSCs and lymphopenia presented by COVID-19 patients. However, future studies are required to test this hypothesis. In conclusion, our integrative systems immunology approach has provided unique insights into the cell cycle alterations that occur during the

FIGURE 8 Cell cycle-associated genes show a strong correlation in severe COVID-19. (A) Correlation analysis of top cell cycle-associated rankers (obtained from random forest analysis: Figure 7B,C) according to COVID-19 severity (COVID-19 and non-COVID-19 [other respiratory illness] cohorts in an intensive care unit [ICU] or not [non_ICU]: from data set GSE157103). The Spearman's rank correlation coefficient is shown according to the color scale bar ranging from -1 to 1. (B) Box plots illustrating the distribution of absolute values (considering all correlation coefficients despite the correlation direction [+ or - sign]) of Spearman correlation coefficients across study cohorts. Each box plot shows the median with the first and third interquartile range (IQR), whiskers representing minimum and maximum values within IQR, and individual data points. Significance was determined using two-sided Wilcoxon rank-sum test and is indicated by asterisks (* $p \leq 0.05$; ** $p \leq 0.01$; *** $p \leq 0.001$, and **** $p \leq 0.0001$). (C) Heatmap of correlation index. The bars aside from the heatmap represent the sum of correlation indexes. The color scale bar represents the correlation index for each gene.

anti-SARS-CoV-2 immune responses. Specifically, this comprehensive systems immunology study identified strong associations between differentially expressed cell-cycle molecules and the severity of COVID-19 that can be explored in therapeutic settings.

AUTHOR CONTRIBUTIONS

Caroline Aliane de Souza Prado, Lena F. Schimke, and Otavio Cabral-Marques supervised the project. Caroline Aliane de Souza Prado, Lena F. Schimke, Otavio Cabral-Marques, Dennyson Leandro M. Fonseca, Youvika Singh, Igor Salerno Filgueiras, Gabriela Crispim Baiocchi, Desirée Rodrigues Praça, Alexandre H. C. Marques, Júlia N. Usuda, Paula Paccielli Freire, Ranieri Coelho Salgado, Sarah Maria da Silva Napoleao, Guangyan Zhou, Neha Mishra, and Igor Jurisica performed bioinformatics analyses. Lena F. Schimke, Gustavo Cabral de Miranda, Vera Lúcia Garcia Calich, Rodrigo Nalio Ramos, Vanderson Rocha, Guangyan Zhou, Rusan Catar, Guido Moll, Niels Olsen Saraiva Camara, Lasse M. Gii, Neha Mishra, Florian Tran, Raquel Costa Silva Dantas-Komatsu, Andre Ducati Luchessi, Helder I. Nakaya, Hans D. Ochs, and Otavio Cabral-Marques provided scientific insights. Lena F. Schimke, Guido Moll, Niels Olsen Saraiva Camara, Vera Lúcia Garcia Calich, Igor Jurisica, Lasse M. Gii, Andre Ducati Luchessi, Hans D. Ochs, and Otavio Cabral-Marques reviewed and edited the final manuscript. Otavio Cabral-Marques conceived and designed the study. Lena F. Schimke and Otavio Cabral-Marques supervised the project.

ACKNOWLEDGMENTS

We thank the São Paulo State Research Support Foundation (FAPESP grants: 2018/18886-9, 2020/01688-0, and 2020/07069-0 to O. C. M.; grant 2020/09146-1 to P. P. F.; 2020/11710-2 to D. R. P.; 2020/16246-2 to D. L. M. F.; 2020/07972-1 to G. C. B.) and the Emergency Action against COVID-19 program established by the Coordination for the Improvement of Higher Education Personnel—Brazil (CAPES) 88887.509891/2020-00 for the financial support. This study was partly financed by CAPES—finance code 001 granted to I. S. F and DS Bridges Scholarship 2021 and National Council for Scientific and Technological Development (CNPq) grant 102430/2022-5 to L. F. S. Computational analysis was supported by FAPESP and partially by the grants from Ontario Research Fund (#34876), Natural Sciences Research Council (NSERC#203475), Canada Foundation for Innovation (CFI #29272, #225404, #33536), and IBM granted to I. J. Contributions of R.C. were made possible by funding from the Deutsche Forschungsgemeinschaft (DFG, German Research Foundation; project #394046635, subproject A03, as part of CRC 1365 and EXPAND-PD; CA2816/1-1). G. M.'s contributions were made possible by the German Research Foundation (DFG; EXPAND-PD CA2816/1-1) and German Federal Ministry of Education and Research (BMBF) funding through the BSRT (GSC203) and BCRT. G. M. received funding from the European Union's Horizon 2020 research and innovation program under grant agreements No 733006 (PACE) and No 779293 (HIPGEN).

CONFLICT OF INTEREST

The authors declare no conflict of interest.

DATA AVAILABILITY STATEMENT

This paper analyzes existing, publicly available data. The accession numbers for the publicly available data sets are listed in the key resources table. R packages are listed in the key resources table and all R codes used for data analysis are available upon reasonable request.

ORCID

Desirée Rodrigues Praça  <http://orcid.org/0000-0002-0305-8289>

Otavio Cabral-Marques  <https://orcid.org/0000-0002-3183-6236>

REFERENCES

- Konings F, Perkins MD, Kuhn JH, et al. SARS-CoV-2 variants of interest and concern naming scheme conducive for global discourse. *Nat Microbiol*. 2021;6(7):821-823. doi:10.1038/s41564-021-00932-w
- Hacisuleyman E, Hale C, Saito Y, et al. Vaccine breakthrough infections with SARS-CoV-2 variants. *N Engl J Med*. 2021;384(23):2212-2218. doi:10.1056/NEJMOA2105000/SUPPL_FILE/NEJMOA2105000_DISCLOSURES.PDF
- Victora CG, Castro MC, Gurmenda S, Medeiros AC, França GVA, Barros AJD. Estimating the early impact of vaccination against COVID-19 on deaths among elderly people in Brazil: analyses of routinely-collected data on vaccine coverage and mortality. *E Clinical Medicine*. 2021;38:101036. doi:10.1016/j.eclinm.2021.101036
- COVID Live. *Coronavirus Statistics*. Worldometer; 2022.
- Brodin P. Immune determinants of COVID-19 disease presentation and severity. *Nature Med*. 2021;27(1):28-33. doi:10.1038/s41591-020-01202-8
- Moll G, Drzeniek N, Kamhieh-Milz J, Geissler S, Volk HD, Reinke P. MSC therapies for COVID-19: importance of patient coagulopathy, thrombocytopenia, cell product quality and mode of delivery for treatment safety and efficacy. *Front Immunol*. 2020;11:1091. doi:10.3389/FIMMU.2020.01091/BIBTEX
- Van Der Made CI, Simons A, Schuurs-Hoeijmakers J, et al. Presence of genetic variants among young men with severe COVID-19. *JAMA*. 2020;324(7):663-673. doi:10.1001/JAMA.2020.13719
- Webb BJ, Peltan ID, Jensen P, et al. Clinical criteria for COVID-19-associated hyperinflammatory syndrome: a cohort study. *Lancet Rheumatol*. 2020;2(12):e754-e763. doi:10.1016/S2665-9913(20)30343-X
- Koutsakos M, Rowntree LC, Hensen L, et al. Integrated immune dynamics define correlates of COVID-19 severity and antibody responses. *Cell Rep Med*. 2021;2(3):100208. doi:10.1016/J.XCRM.2021.100208
- Asano T, Boisson B, Onodi F, et al. X-linked recessive TLR7 deficiency in ~1% of men under 60 years old with life-threatening COVID-19. *Sci Immunol*. 2021;6(62):eabd4348. doi:10.1126/SCIIMMUNOL.ABL4348/SUPPL_FILE/SCIIMMUNOL.ABL4348_DATA_FILES.S1_TO_S7.ZIP
- Zhang Q, Bastard P, Liu Z, et al. Inborn errors of type I IFN immunity in patients with life-threatening COVID-19. *Science*. 2020;370(6515):eabd4570. doi:10.1126/SCIENCE.ABD4570
- Cabral-Marques O, Halpert G, Schimke LF, et al. Autoantibodies targeting GPCRs and RAS-related molecules associate with COVID-19 severity. *Nat Commun*. 2022;13(1):1220. doi:10.1038/s41467-022-28905-5
- Wang EY, Mao T, Klein J, et al. Diverse functional autoantibodies in patients with COVID-19. *Nature*. 2021;595(7866):283-288. doi:10.1038/s41586-021-03631-y
- Lourda M, Dzidic M, Hertwig L, et al. High-dimensional profiling reveals phenotypic heterogeneity and disease-specific alterations of granulocytes in COVID-19. *Proc Natl Acad Sci*. 2021;118(40):e2109123118. doi:10.1073/PNAS.2109123118/-/DCSUPPLEMENTAL

15. Bouhaddou M, Memon D, Meyer B, et al. The global phosphorylation landscape of SARS-CoV-2 infection. *Cell*. 2020;182(3):685-712. doi:10.1016/J.CELL.2020.06.034
16. Fan Y, Sanyal S, Bruzzone R. Breaking bad: how viruses subvert the cell cycle. *Front Cell Infect Microbiol*. 2018;8:396. doi:10.3389/fcimb.2018.00396
17. Yoder AC, Guo K, Dillon SM, et al. The transcriptome of HIV-1 infected intestinal CD4+ T cells exposed to enteric bacteria. *PLoS Pathog*. 2017;13(2):e1006226. doi:10.1371/journal.ppat.1006226
18. Su M, Chen Y, Qi S, Shi D, Feng L, Sun D. A mini-review on cell cycle regulation of coronavirus infection. *Front Vet Sci*. 2020;7:943. doi:10.3389/FVETS.2020.586826/BIBTEX
19. Nascimento R, Parkhouse RME. Murine gammaherpesvirus 68 ORF20 induces cell-cycle arrest in G2 by inhibiting the Cdc2-cyclin B complex. *J Gen Virol*. 2007;88(pt 5):1446-1453. doi:10.1099/VIR.0.82589-0
20. Coleman ML, Marshall CJ, Olson MF. RAS and RHO GTPases in G1-phase cell-cycle regulation. *Nat Rev Mol Cell Biol*. 2004;5(5):355-366. doi:10.1038/nrm1365
21. Li L, Gu B, Zhou F, et al. Human herpesvirus 6 suppresses T cell proliferation through induction of cell cycle arrest in infected cells in the G2/M phase. *J Virol*. 2011;85(13):6774-6783. doi:10.1128/JVI.02577-10/FORMAT/EPUB
22. Palmisano A, Zámorsky J, Oguz C, Csikász-Nagy A. Molecular network dynamics of cell cycle control: periodicity of start and finish. *Methods Mol Biol*. 2017;1524:331-349. doi:10.1007/978-1-4939-6603-5_21
23. Schimke LF, Marques AHC, Baiocchi GC, et al. Severe COVID-19 shares a common neutrophil activation signature with other acute inflammatory states. *Cells*. 2022;11(5):847. doi:10.3390/cells11050847
24. Sanchis P, Lavignolle R, Abbate M, et al. Analysis workflow of publicly available RNA-sequencing datasets. *STAR Protoc*. 2021;2(2):100478. doi:10.1016/j.xpro.2021.100478
25. Zhou G, Soufan O, Ewald J, Hancock REW, Basu N, Xia J. NetworkAnalyst 3.0: a visual analytics platform for comprehensive gene expression profiling and meta-analysis. *Nucleic Acids Res*. 2019;47(W1):W234-W241. doi:10.1093/nar/gkz240
26. Love MI, Anders S, Kim V, Huber W. RNA-Seq workflow: gene-level exploratory analysis and differential expression. *F1000Res*. 2015;4:1070. doi:10.12688/f1000research.7035.1
27. Akgun E, Tuzuner MB, Sahin B, et al. Proteins associated with neutrophil degranulation are upregulated in nasopharyngeal swabs from SARS-CoV-2 patients. *PLoS One*. 2020;15(10):e0240012. doi:10.1371/JOURNAL.PONE.0240012
28. Huo Z, Tang S, Park Y, Tseng G. P-value evaluation, variability index and biomarker categorization for adaptively weighted Fisher's meta-analysis method in omics applications. *Bioinformatics*. 2020;36(2):524-532. doi:10.1093/bioinformatics/btz589
29. Sander J, Schultze JL, Yosef N. ImpulseDE: detection of differentially expressed genes in time series data using impulse models. *Bioinformatics*. 2017;33(5):757-759. doi:10.1093/BIOINFORMATICS/BTW665
30. Bernardes JP, Mishra N, Tran F, et al. Longitudinal multi-omics analyses identify responses of megakaryocytes, erythroid cells, and plasmablasts as hallmarks of severe COVID-19. *Immunity*. 2020;53(6):1296-1314. doi:10.1016/J.IMMUNI.2020.11.017
31. Overmyer KA, Shishkova E, Miller IJ, et al. Large-scale multi-omic analysis of COVID-19 severity. *Cell Syst*. 2021;12(1):23-40. doi:10.1016/J.CELS.2020.10.003
32. Arunachalam PS, Wimmers F, Mok CKP, Perera RAPM, et al. Systems biological assessment of immunity to mild versus severe COVID-19 infection in humans. *Science*. 2020;369(6508):1210-1220.
33. Satyanarayana A, Kaldis P. Mammalian cell-cycle regulation: several Cdk, numerous cyclins and diverse compensatory mechanisms. *Oncogene*. 2009;28(33):2925-2939. doi:10.1038/ncr.2009.170
34. Foli A, Maiocchi MA, Lisiewicz J, Lori F. A checkpoint in the cell cycle progression as a therapeutic target to inhibit HIV replication. *J Infect Dis*. 2007;196(9):1409-1415. doi:10.1086/521832
35. Meijer L. Cyclin-dependent kinases inhibitors as potential anticancer, antineurodegenerative, antiviral and antiparasitic agents. *Drug Resist Updates*. 2000;3(2):83-88. doi:10.1054/DRUP.2000.0129
36. Barnum KJ, O'Connell MJ. Cell cycle regulation by checkpoints. *Methods Mol Biol*. 2014;1170:29. doi:10.1007/978-1-4939-0888-2_2
37. Mizrahi B, Lotan R, Kalkstein N, et al. Correlation of SARS-CoV-2 breakthrough infections to time-from-vaccine. *Nat Commun*. 2021;12(1):6379. doi:10.1038/s41467-021-26672-3
38. Liu HL, Yeh IJ, Phan NN, et al. Gene signatures of SARS-CoV/SARS-CoV-2-infected ferret lungs in short- and long-term models. *Infect Genet Evol*. 2020;85:104438. doi:10.1016/J.MEEGID.2020.104438
39. Ferreira FL, Bota DP, Bross A, Mélot C, Vincent JL. Serial evaluation of the SOFA score to predict outcome in critically ill patients. *JAMA*. 2001;286(14):1754-1758. doi:10.1001/JAMA.286.14.1754
40. Prozan L, Shusterman E, Ablin J, et al. Prognostic value of neutrophil-to-lymphocyte ratio in COVID-19 compared with influenza and respiratory syncytial virus infection. *Sci Rep*. 2021;11(1):21519. doi:10.1038/s41598-021-00927-x
41. Crevel R. Lymphocyte proliferation. In: *Encyclopedic Reference of Immunotoxicology*. Springer; 2005:401-405. doi:10.1007/3-540-27806-0_920
42. Yang L, Liu S, Liu J, et al. COVID-19: immunopathogenesis and immunotherapeutics. *Signal Transduct Target Ther*. 2020;5(1):128. doi:10.1038/s41392-020-00243-2
43. Wang X, Wen Y, Xie X, et al. Dysregulated hematopoiesis in bone marrow marks severe COVID-19. *Cell Discov*. 2021;7(1):60. doi:10.1038/s41421-021-00296-9
44. Wang J, Jiang M, Chen X, Montaner LJ. Cytokine storm and leukocyte changes in mild versus severe SARS-CoV-2 infection: review of 3939 COVID-19 patients in China and emerging pathogenesis and therapy concepts. *J Leukoc Biol*. 2020;108(1):17-41. doi:10.1002/JLB.3COVR0520-272R
45. Condamine T, Gabrilovich DI. Molecular mechanisms regulating myeloid-derived suppressor cell differentiation and function. *Trends Immunol*. 2011;32(1):19-25. doi:10.1016/j.it.2010.10.002
46. Schulte-Schrepping J, Reusch N, Paclik D, et al. Severe COVID-19 is marked by a dysregulated myeloid cell compartment. *Cell*. 2020;182(6):1419-1440.e23. doi:10.1016/j.cell.2020.08.001
47. Silvén A, Chapuis N, Dunsmore G, et al. Elevated calprotectin and abnormal myeloid cell subsets discriminate severe from mild COVID-19. *Cell*. 2020;182(6):1401-1418.e18. doi:10.1016/j.cell.2020.08.002
48. Agrati C, Sacchi A, Bordoni V, et al. Expansion of myeloid-derived suppressor cells in patients with severe coronavirus disease (COVID-19). *Cell Death Differ*. 2020;27:3196-3207. doi:10.1038/s41418-020-0572-6
49. Gabrilovich DI, Nagaraj S. Myeloid-derived suppressor cells as regulators of the immune system. *Nat Rev Immunol*. 2009;9(3):162-174. doi:10.1038/nri2506

SUPPORTING INFORMATION

Additional supporting information can be found online in the Supporting Information section at the end of this article.

How to cite this article: Prado CADs, Fonseca DLM, Singh Y, et al. Integrative systems immunology uncovers molecular networks of the cell cycle that stratify COVID-19 severity. *J Med Virol*. 2023;95:e28450. doi:10.1002/jmv.28450